ACS Sustainable Chemistry & Engineering

pubs.acs.org/journal/ascecg

Research Article

Developing Decision-Making Tools for Food Waste Management via Spatially Explicit Integration of Experimental Hydrothermal Carbonization Data and Computational Models Using New York as a Case Study

Nazih Kassem, Matteo Pecchi, Alex R. Maag, Marco Baratieri, Jefferson W. Tester, and Jillian L. Goldfarb*

Cite This: *ACS Sustainable Chem. Eng.* 2022, 10, 16578−16587

Read Online

ACCESS | Metrics & More | Article Recommendations | Supporting Information

ABSTRACT: Food systems account for one third of all global anthropogenic greenhouse gas emissions, and food waste (FW) produces one third of landfill emissions in the U.S. To combat global warming, we must upcycle FW by developing closed-loop supply chains—key features of a circular economy—that harmonize technology and policies. New York State (NYS) recently enacted a law requiring generators of >1.8 t/week to redirect FW from landfills to processing centers within 40.2 km of the waste generation. Hydrothermal carbonization could transform FW into a coal-like solid fuel, but there is scant information on the feasibility of implementing this approach under current policy conditions. We developed a model informed by experimental results to evaluate the interplay between HTC plant location, feedstock availability, policies, and economic viability within NYS. Broadly, this is a case study of a new decision-making tool enabling policy makers and entrepreneurs alike to plan effective resource valorization.

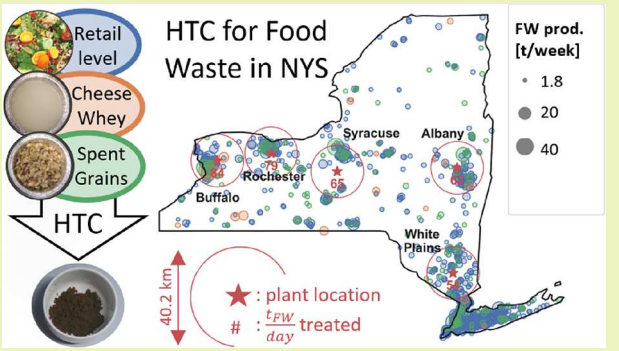

KEYWORDS: *food waste, biorefinery, GIS model, techno-economic analysis, hydrothermal carbonization, GHG emissions, policy*

INTRODUCTION

From seed to supermarket, food systems are responsible for a third of global anthropogenic greenhouse gas (GHG) emissions.[1] The United States (U.S.) generates over 60 million tons of food waste (FW) annually. FW is the largest component of municipal solid waste (MSW) landfills,[2] which in turn are the third largest source of anthropogenic methane emissions in the U.S.[3] We must develop a closed-loop circular economy that is synergistically supported by advances in policies and technology[4] to mitigate food system impacts. Climate-centric policies that incentivize or require FW valorization will only succeed if policy, investment, and technological developments align toward efficient resource use.[5]

Policy makers and entrepreneurs alike need accurate tools to inform decision-making. For waste valorization schemes, this means understanding feedstock availability as a function of location and conversion pathways and products for the specific feedstocks. In 2022, New York State (NYS) enacted the Food Donation and Food Scraps Recycling law, requiring commercial producers of more than 1.8 metric ton (t) per week (2 US short tons/week) of FW within 40.2 km (25 miles) of a treatment facility to redirect their wastes from landfills.[6] Many landfills across NYS will close by 2050, while MSW generation will increase concomitantly;[7] this steady supply of waste feedstocks creates opportunities for commercialization of FW conversion technologies.

Common FW management pathways include combustion and anaerobic digestion (AD). Combustion is limited by its (1) energy recovery efficiency due to FW's high moisture content and (2) generation of air pollutants.[8] Although AD is a suitable treatment option for wet organic feedstocks, it requires long residence times. FW's high organic loading accumulates volatile fatty acids that can inhibit the digester's microbial activity and produces an often undesired digestate.[9−11] Avoiding inhibition requires the addition of a buffer such as manure, which limits the potential locations for FW processing plants. The lack of a suitable treatment facility negates the NYS

Received: July 13, 2022
Revised: November 17, 2022
Published: December 5, 2022

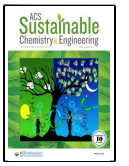

requirement for FW redirection, begging the question: what future options are available to treat FW with short residence times and enhanced carbon recovery?

Hydrothermal carbonization (HTC) converts wet biomass into a coal-like solid hydrochar (HC) in water, negating the need for an energy-intensive drying pretreatment step. It occurs in minutes (versus days for AD).[12] During HTC, biomass is heated between 180 and 250 °C at pressures of 2 to 10 MPa,[13] producing a gas comprised mainly of CO_2, an organic-rich aqueous phase, and a HC.[14] Suggested HC uses include as a fuel for energy generation[15] or as a soil amendment.[16] However, as many as-carbonized HCs contain phytotoxic compounds,[17] HC use as a fuel is investigated here.

Most techno-economic analyses (TEAs) on HTC are based on literature data for generic locations or feedstocks "similar" to a studied location. Such studies consider "functional unit" feedstock inflows in their models[18−22] such as a recent analysis of a fixed-size hypothetical industrial-scale plant processing olive pruning,[18] which may not represent implementable HTC conditions. Other analyses fix pre-determined locations with specific feedstock rates based on local assessments[23−25] or aggregate spatial data into regional averages.[24] Medina-Martos et al.[26] examined the coupling of HTC as a secondary step to treat wastewater sludges in existing plants.[26] In a TEA of HTC for sewage management, inflow rates were estimated based on populations in the study region, assuming fixed distances between households,[24] limiting widespread applicability. Saba et al.[27] sized an HTC plant based on a coal power plant's electric output.[27] Such models are therefore constrained with a specific feed rate. Shahid and Hittinger[28] address these issues by looking at the techno-economic optimization of FW diversion using anaerobic co-digestion as it relates to NYS's FW law and spatially dependent feedstock profile. To our knowledge, no prior HTC TEA integrates granular feedstock geographic data to assess the spatial performance of HTC plants at a regional level, let alone in light of FW diversion regulations (e.g., eligibility of FW producers and distance to nearest treatment facility) on system performance. To fill this gap, we developed a geographic information system (GIS)-based model to evaluate the performance of hypothetical HTC plants processing FW across NYS. The model incorporates experimental HTC data on the process performance of specific available feedstocks to understand the HC yield and energy recovery as a function of FW producer location. We use the model to evaluate the interplay between the HTC plant location, feedstock availability, policies, and economic viability in NYS as a case study to develop new experimentally informed GIS-TEA models as decision-making tools for policy makers and entrepreneurs alike.

MATERIALS AND METHODS

We identified the largest sources of FW in NYS and mapped them using geographic coordinates using the New York State Pollution Prevention Institute Organic Resource Locator database[29] as described previously.[30] Supermarkets, restaurants, and universities were grouped as a single category (SRU) because of their similar waste compositions and concentrated urban locations. Brewery waste (brewers' spent grains: BSG) and dairy waste (dairy cheese whey: DCW) have localized production and uniform composition. While bakeries represent a significant FW source, the only bakery waste generators subject to the new FW disposal regulation are concentrated around New York City and a large portion of this "waste" is viable food that can be inserted into donation networks such that HTC is not a preferred management strategy. All input data was converted into SI units. Costs were converted to US dollars ($) using currency exchange rates of the year the data were reported.

Spatial Modeling and Waste Allocation. In accordance with the NYS FW law, our waste allocation model redirects FW into centralized HTC plants with coordinates specified based on each individual FW producer's generation rates and Euclidian distances to the proposed plant. The use of Euclidian distances introduces some error in transportation cost estimates. However, transportation has but a minor impact on the economics and GHG emissions balance given the small buffer radius, justifying this simplification. Only FW producers that meet the minimum waste throughput $\dot{m}_{min}$ (t/week) as required by NYS policies and are within the specified buffer radius r_{buffer} (km) of the plant allocated are included. The total influent feedstock flow rate is used as a basis for mass balances and economic calculations. To visualize the spatial performance of hypothetical HTC plants, the waste allocation model calculations were iterated over hypothetical plant coordinates in a 100 × 100 grid across NYS. The grid is bounded by NYS's spatial coordinates, spanning a longitude of −80 to −72 and a latitude of 40−45 and distances of 681 and 555 km, respectively, such that (Δx = 6.8 km) and (Δy = 5.5 km). This resolution provides sufficient granularity to visualize the spatial variation of selected performance metrics and identify optimal plant locations (based on maximized or minimized target metrics).

Hydrothermal Carbonization of GIS-Identified Food Waste Mixtures. A detailed description of the FW samples is reported in Pecchi et al.[31] Briefly, the SRU feedstock mixture was produced by blending commonly disposed consumer food items in representative FW ratios. BSG was obtained from a local brewery in Ithaca, NY; dairy cheese whey (DCW) was sourced from the Cornell Dairy.

HTC experiments were performed as documented previously.[31] Three temperatures, T_{HTC} (190, 220, and 250 °C), and two reaction times, $time_{HTC}$ (1 and 3 h), were investigated to assess their impact on the HC yield (Y_{HC}, % dry mass), HC heating value (HHV_{HC}, MJ/kg), and gas yield (Y_{gas}, % dry mass) of single FW streams and select mixtures. Mixture ratios were determined according to GIS feedstock mapping to represent available biomass at a given location. Water was added to SRU and BSG feedstocks to reach an HTC feed moisture content of 85 wt %, while DCW was used as-is (95 wt % moisture). Water was added to mixtures with moisture contents of <85 wt % as per eq 1; mixtures where DCW increased the total water content above 85 wt % were carbonized as mixed.

$$\frac{Q_{water,total}}{Q_{HTC,total}} = \frac{(Q_{feedstock} \times mc_{feedstock}) + water_{add}}{Q_{feedstock} + water_{add}} = mc_{target} \quad (1)$$

$Q_{feedstock}$ represents the feedstock mixture flow rate (t/day), $water_{add}$ is additional water (t/day), $Q_{HTC,\ total}$ is the total flow rate (t/day) entering the reactor, and $mc_{feedstock}$ and mc_{target} the feedstock mixture and target moisture content (wt %), respectively.

Mass and Energy Balances. HC generation (HC_{gen}, t/day) as a function of reaction temperature and residence time is computed based on solids recovered from HTC experiments:

$$HC_{gen} = \bar{Y}_{HC} \cdot (Q_{feedstock} + water_{add}) \cdot (1 - mc_{target}) \quad (2)$$

Energy generation (E_{gen}, MJ/day) and energy recovery (ER, %) for a given feedstock mixture (at T_{HTC} and $time_{HTC}$) are computed via eqs 3 and 4, where $HHV_{feedstock}$ is the geometric average of the feedstock mixture's higher heating value.

$$E_{gen} = HC_{gen} \cdot \overline{HHV}_{HC} \quad (3)$$

$$ER = \frac{E_{gen}}{Q_{feedstock} \cdot (1 - mc_{feed}) \cdot HHV_{feedstock}} \quad (4)$$

The produced aqueous phase flow rate (Q_{AP}, t/day) was computed using eq 5 where Q_{gas} is the gaseous phase mass rate (t/day).

$$Q_{AP} = Q_{HTC,total} - HC_{gen} - Q_{gas} \quad (5)$$

https://doi.org/10.1021/acssuschemeng.2c04188
ACS Sustainable Chem. Eng. 2022, 10, 16578−16587

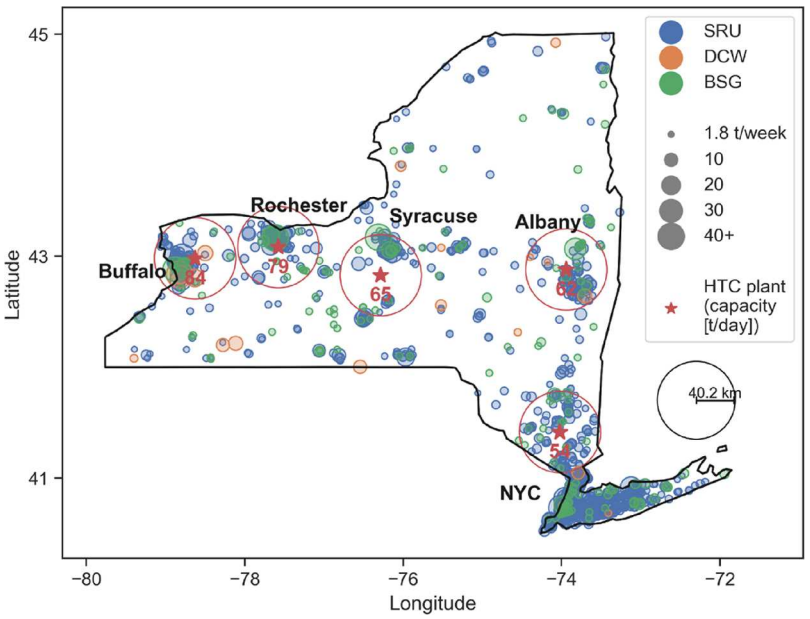

Figure 1. Waste feedstock spatial distribution. Feedstocks are displayed for producers generating more than 1.8 t/week. Weekly amounts are indicated by the size of the dot, while the color identifies the type of waste (SRU: supermarkets, restaurants, and universities, BSG: brewery spent grains, and DCW: dairy cheese whey). The figure also shows the best non-overlapping five HTC plant locations that result in the lowest emissions in the base case.

Cost Estimation. An HTC capital cost curve ($CAPEX_{HTC}$ [US$], eq 6) as a function of wet HTC processing capacity ($Q_{HTC,\ wet}$ [t/y]) was estimated by fitting literature CAPEX and HTC wet mass rate data;[19,22,26,32] a comparison with different fitting approaches is available in Figure S1.

$$CAPEX_{HTC} = 7{,}430{,}519 + \left(\frac{Q_{HTC,wet}}{2.81 \times 10^{-7}}\right)^{0.6} \quad (6)$$

The working capital (WC) for startup and construction was set at 5% of CAPEX, which was incurred at the end of construction period.

Operating costs comprise both fixed and variable costs. Fixed costs (FCs) include supervision, overhead, labor, maintenance, and tax and are calculated using the methodology as detailed by Michailos et al.[33] by adopting the average rate for NYS chemical plant operators.[34] Variable costs (VC) consist of utilities (electric and heat), transportation, and aqueous phase disposal costs. HTC cost factors (kWh/kg feedstock) were estimated from Fiori et al.[20] (Table S2). Utility costs are calculated based on NYS annual average industrial retail prices.[35,36]

Transportation costs are computed based on feedstock generation rates and distances between producers and proposed HTC plant locations. For solids (SRU and BSG), transportation costs are calculated per kilometer for 20 t capacity long-haul trucks.[37] For liquids (DCW), transportation costs are estimated from the hauling rate of 40.9 m^3 (9000 gal) tanker trucks.[38] Yearly hauling time (h/y) is estimating through the number of truck-trips (trips/y), while the h per trip accounts for driving, loading, and unloading time. The aqueous phase disposal cost is based on industrial wastewater treatment data for the Syracuse water authority.[39] Details on operating costs estimation methods and parameters are summarized in Table S3.

The HTC plant generates two revenue streams: HC sold as a solid fuel to substitute for low-rank coals and tipping fees. Although NYS stopped using coal in the electric power sector as of 2020,[40] biomass-derived HC can be exported to power plants in nearby states such as Pennsylvania. The US average lignite coal price of $16.50/t[41] and NYS average landfilling fee of $78.1/t[42] were assumed for HC and tipping fee revenues, respectively.

Discounted Cash Flow Analysis. After all costs (CAPEX, FC, VC, and WC) and revenue streams associated with the HTC plant were determined, a discounted cash flow (DCF) analysis was performed to compute economic performance metrics for the HTC plant (model development available in the Supporting Information). The net present value (NPV) measures the financial returns net of capital investments and operating costs, while the HC minimum selling price (MSP_{HC}) represents the minimum HC selling price ($/t) required to breakeven at the end of the project lifetime and is a measure of the potential market competitiveness of the HC as a solid fuel. The MSP_{HC} can be reduced by revenue generated through tipping fees. As such, the $MSP_{HC,eff}$ denotes the effective MSP_{HC} and is calculated using eq 7 where $R_{tipping\ fees}$ represents the annual tipping fees revenues ($/y) and $HC_{gen,\ annual}$ is the annual HC generation (t/y). The fraction on the right side of the equation normalizes the tipping fee revenues per ton of HC generated. A negative $MSP_{HC,eff}$ denotes net profits where tipping fee revenues alone result in breakeven conditions.

$$MSP_{HC,eff} = MSP_{HC} - \frac{R_{tipping\ fees}}{HC_{gen,annual}} \quad (7)$$

A cash flow diagram showing all cash flow components of the DCF model across the project lifetime is found in Figure S2.

Greenhouse Gas Emission Estimation. Emissions result from utility consumption, transportation, and process emissions; avoided emissions include FW landfilling and coal displacement. The average landfilling emission factor was calculated using the EPA's Landfill Methane Outreach Program (LMOP) database[43] (Tables S5 and S6). This factor accounts for direct CH_4, CO_2, and oxidized CH_4 emissions from unrecovered landfill gas and CO_2 emissions from flaring landfill gas. The 2020 NYS electric grid emission factor was based on the eGRID database,[44] which accounts for the actual fuel mix used in NYS's electric power sector. The natural gas (NG) carbon intensity was calculated based on 2018 NYS NG-associated CO_2 emission and consumption data.[45,46] Transportation emissions were calculated using CO_2, N_2O, and CH_4 emission factors for mobile combustion of diesel heavy-duty vehicles[47] as a function of the annual feedstock hauling distance. The 100-year GWP of 28 and 265 for CH_4 and N_2O were assumed in the calculations of $CO_{2,eq}$ emissions.[48] The avoided emissions from the substitution of coal by HC were estimated based on 2019 coal emission and production data from 658 U.S. coal mines.[49] Emission factors are available in Table S7. The HTC plant's

https://doi.org/10.1021/acssuschemeng.2c04188
ACS Sustainable Chem. Eng. 2022, 10, 16578−16587

Table 1. Feedstock Properties[31] and Descriptive Statistics of Three FW Feedstocks Available in NYS[a]

feedstock	moisture (wt %)	HHV (MJ/kg)	density (kg/m^3)	frequency (no. of generators)	average gen. rate (t/week)	min. gen. rate (t/week)	max. gen. rate (t/week)
SRU	52.8	26.0	452	1014	4.3	1.8	48.1
DCW	94.9	18.5	1000	19	8.6	2.0	35.9
BSG	68.7	19.7	432	177	5.5	2.1	159.4

[a]Statistics displayed are for FW producers generating more than 1.8 t/week.

Table 2. Experimental HC and Gas Yield (Y_{HC} and Y_{gas}) and HHV of HC (HHV_{HC}) for SRU, DCW, and BSG Feedstocks and Mixtures[a]

	fraction of feedstock (dry basis wt %)				Y_{HC} (wt %)			Y_{gas} (wt %)			HHV_{HC}(MJ/kg)		
					T_{HTC} (°C)								
feed	SRU	DCW	BSG	time$_{HTC}$ (hr)	190	220	250	190	220	250	190	220	250
SRU	100			1	48.1	56.9	56.2 ± 1.4	1.6	3.5	4.6 ± .3	34.9	34.8	35.9
	100			3	54.3	58.8	59.9	2.5	4.7	4.5	34.4	35.3	36.2
DCW		100		1	23.5	35.0	35.0	2.8	6.8	9.4	28.4	28.9	30.1
		100		3	35.7	32.7	36.8	5.1	7.9	10.2	28.0	28.8	30.2
BSG			100	1	42.8	52.1	47.8	2.2	4.9	6.4	26.3	28.5	30.2
			100	3	54.6	51.9 ± 1.2	50.3	3.7	5.9 ± 0.1	7.7	27.2	29.1	31.8
mix 1	90.2	9.8		1	51.6		58.9				35.1		35.2
calculated value (3q 1)					45.7		55.8				34.3		35.4
% difference (synergistic effect)					11%		5%				2%		0%
mix 2	60.1		39.9	1	47.6		57.7				32.0		34.2
calculated value (eq 1)					46.0		53.9				31.5		33.7
% difference (synergistic effect)					3%		6%				2%		1%
mix 3		14.0	86.0	1	43.7		48.1				27.0		30.6
calculated value (eq 1)					40.1		46.0				26.6		30.2
% difference (synergistic effect)					8%		4%				2%		1%
mix 4	56.4	6.1	37.5	1	49.8		55.2				32.1		34.1
calculated value (eq 1)					44.6		52.8				31.3		33.4
% difference (synergistic effect)					10%		4%				2%		2%

[a]Tests with SRU at 250 °C-1 h and BSG 220 °C-3 h were triplicated, and the average and standard deviation for Y_{HC} and Y_{gas} are shown. HTC results using mixtures created on 0.5/0.5 or 0.33/0.33/0.33 wet fractions of each FW type; data reported with the dry content of each feedstock.

annual net emissions (t $CO_{2,eq}$/y) were calculated using eq 8, where negative terms represent avoided emissions.

$$\text{net } CO_2 \text{ emissions} = CO_{2,\text{electric}} + CO_{2,\text{heat}} + CO_{2,\text{transport}} + CO_{2_{HTC}} - CO_{2,\text{landfill}} - CO_{2,\text{coal}} \quad (8)$$

Carbon intensity (CI, t $CO_{2,eq}$/t) of the produced HC was calculated by dividing annual net emissions by annual HC production.

RESULTS AND DISCUSSION

The three largest sources of FW across NYS were identified and mapped using geographic coordinates (Figure 1) using the NYS Pollution Prevention Institute Organic Resource Locator database.[29] Table 1 shows that the number of generators (meeting the $\dot{m}_{min}$ 1.8 t/week constraint) is dominated by SRU. Outliers include large brewing companies such as Anheuser Busch, Inc., and North American Breweries with estimated BSG generation rates of 160 and 73 t/week, respectively. DCW producers are located in regions near Concentrated Animal Feeding Operation (CAFO) farms. The moisture content, density, and higher heating value (HHV) of the feedstocks (previously determined) are displayed in Table 1.

Hydrothermal Carbonization of GIS-Identified Feedstocks. HTC of the three feedstocks and their mixtures produces solid fuels with energy contents greater than of low-rank lignite coals using even mild HTC conditions (190 °C, 1 h). The results (Table 2) suggest synergistic effects for mixtures concentrated in SRU in terms of enhanced solid yields and HHVs greater than predicted by a weighted average of feedstocks. Such synergy is noted in the literature for some feedstocks with additive behavior for other biomasses.[50] Overall, the degree of synergy was less than 12% for all mixtures across conditions with synergy decreasing for most mixtures as the HTC temperature increases. However, given that the percent synergism is similar to the standard deviation of the replicated trials, the statistical significance of this synergy (and its low effect) led us to compute Y_{HC}, Y_{gas}, and HHV_{HC} for mixtures of different feedstocks using geometric averages of single-feedstock values according to eq 9. The use of weighted

https://doi.org/10.1021/acssuschemeng.2c04188
ACS Sustainable Chem. Eng. 2022, 10, 16578−16587

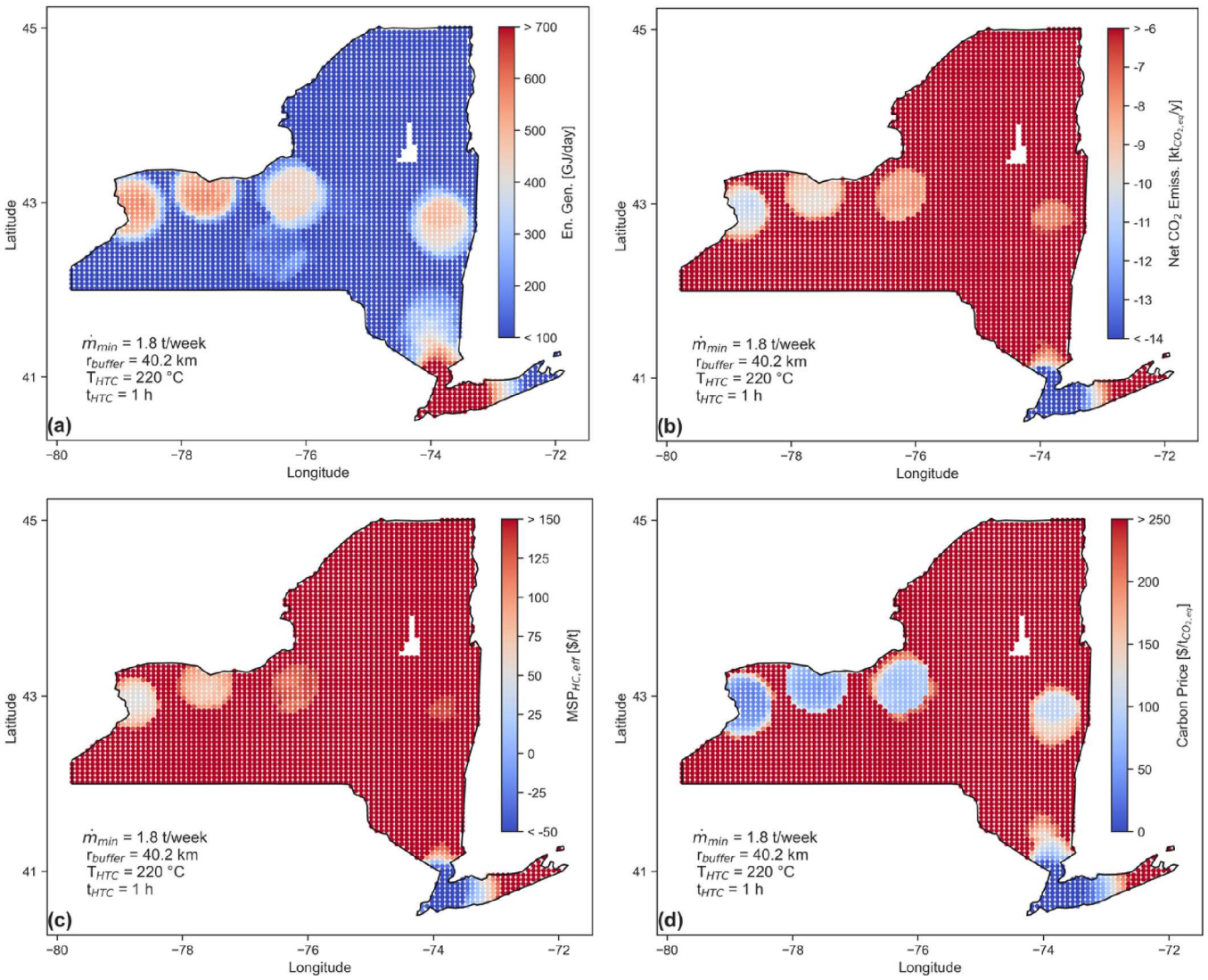

Figure 2. Spatial variations in NYS of (a) energy generation, (b) net CO_2 emissions, (c) $MSP_{HC,eff}$, and (d) competitive carbon prices for HTC biorefineries under base case assumptions. Each 'pixel' represents a hypothetical HTC plant in the 100 × 100 grid.

averages may modestly underpredict the solid yield and energy content, rendering a conservative overall revenue generation calculation. However, the sensitivity analysis varying reaction conditions and policy instrument implications demonstrate the direction in which the reaction synergy would affect the system's economics.

$$\overline{X} = \left.\frac{\sum_{n=1}^{3} X_n \cdot \dot{m}_n}{\sum_{n=1}^{3} \dot{m}_n}\right|_{T_{\mathrm{HTC}},\mathrm{time}_{\mathrm{HTC}}} \quad (9)$$

$\overline{X}$ represents the average mixture value, X_n is the single feedstock value for Y_{HC}, Y_{gas}, and HHV_{HC} at the given T_{HTC} and $time_{HTC}$, and $\dot{m}_n$ is the mass rate (t/day) of feedstock n.

Spatial Analysis of HTC for FW Management. HTC at 220 °C, 1 h, was chosen for the initial base case operating conditions (Table S8) to survey the potential energy recovery and environmental tradeoffs of a network of distributed HTC biorefineries across NYS. This base case used existing regulatory constraints, whereby plants generating 1.8 t/week or more of FW ($\dot{m}_{min}$) within a 40.2 km r_{buffer} are required to treat their FW if a facility is available to take the waste.

Energy generation potential is greater in urban areas (Figure 2a) due to a high density of FW producers. For example, an HTC plant near Rochester (latitude 43.08, longitude −77.57) processing 79 t/day (63% SRU, 0% DCW, and 37% BSG) within a 40.2 km radius could generate 586,000 MJ/day of HC-based combustion energy, representing a 55% energy recovery. This is equivalent to generating 20 GWh/y of electricity (assuming 33% coal plant electric efficiency[51]). By comparison, the 2020 Downstate electricity production was 66,960 GWh/y.[52] Although this HTC plant's energy output is small by comparison, it results in a net emission reduction of 9.99 kt $CO_{2,eq}$/y (Figure 2b). Avoided landfilling emissions contribute the majority of the emissions reduction (−15.8 kt $CO_{2,eq}$) followed by avoided coal mining emissions (−0.5 kt $CO_{2,eq}$). Positive emission contributions include HTC heat imports (+5.1 kt), electricity imports (+0.7 kt $CO_{2,eq}$), HTC process gas (+ 0.5 kt $CO_{2,eq}$), and transportation (+0.02 kt $CO_{2,eq}$) (Figure 3a). The small impact of wet FW transportation—compared to the other parameters—on the overall economic and environmental performance of the biorefinery suggests an even smaller impact of dry HC transportation to

https://doi.org/10.1021/acssuschemeng.2c04188
ACS Sustainable Chem. Eng. 2022, 10, 16578−16587

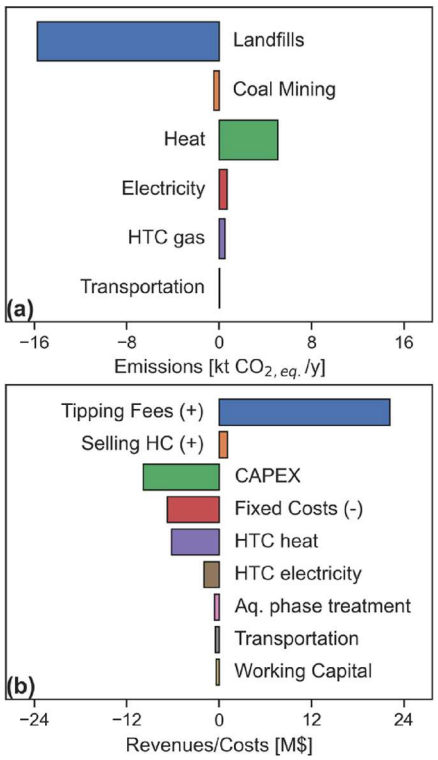

Figure 3. Emissions (a) and NPV (b) breakdown for the Rochester HTC plant. All cost/revenue values displayed in b represent the present value of each cost/revenue components such that their sum equals to the NPV.

the nearest coal plant. HC transportation was therefore neglected.

NYS's electric power sector emissions totaled 27 Mt of $CO_{2,eq}$ in 2020,[44] while GHG emissions from NYS landfills amounted to 10.6 Mt $CO_{2,eq}$ in 2016.[53] As a comparison, an HTC plant in the NYC area (40.70, −73.85) would process 249 t FW/day, generating 73 GWh/y of electricity with a net emissions reduction of 30 kt $CO_{2,eq}$/y. However, NYC has its own FW diversion laws and complex FW transportation logistics; this is illustrative only of the potential for HTC to manage FW in highly populated areas.

Spatial Variability in Base Case Economic Considerations. Beyond energy and environmental benefits, project costs are key considerations when assessing economic feasibility. Figure 2c shows the $MSP_{HC,\,eff}$ under base case assumptions. The NPV (Figure S3) is positive at locations where the $MSP_{HC,eff}$ is below the HC selling price of $16.5/t (Figure 2c). With current lignite coal prices and no carbon credits or subsidies, only NYC area HTC biorefineries would have a sufficient scale to recover capital investment and generate profits. Further afield, lower FW generation plus high capital costs and low HC selling prices yield negative NPVs. The slightly higher (but still negative) NPVs found in urban areas correlate with the increased FW density. As an example, the NPV at the Rochester plant is −3 M$. Without financial incentives, the NPV contribution from tipping fees (22 M$) and HC (1 M$) revenues are not sufficient to recover the total capital (10 M$), operating costs (16 M$), and working capital (0.4 M$) as shown by the NPV breakdown in Figure 3b. Figure 2c illustrates the magnitude of economic incentives needed to produce positive NPVs at a given plant location. For example, the $MSP_{HC,eff}$ at an HTC plant in Rochester (43.080, −77.575) is $65/t. A financial incentive of at least $48.5/$t_{HC}$ is required for the plant to breakeven; HC breakeven selling prices in the literature range from $30 to $226/t.[20,23,27]

Carbon Intensity Considerations to Aid Policy Decision-Making. Our model provides policy makers quantitative data regarding the magnitude of funds needed for carbon mitigation projects as a tool for energy planning. The HC incentive of $48.5/t could be tied to carbon offsets. The calculated CI_{HC} for hypothetical HTC biorefineries is negative across NYS (Figure S4), while the average emission factor for coal produced in US mines is 0.074 t $CO_{2,eq}$/t[49]. This suggests that HC production is an effective carbon mitigation strategy when used as a substitute for lignite coal.

Competitive carbon prices ($/t $CO_{2,eq}$) were calculated using $MSP_{HC,eff}$ and CI_{HC} values. As an example, the HC produced at the Rochester plant has a CI of −1.51 t $CO_{2,eq}$/t HC. Given an $MSP_{HC,eff}$ of $65/t HC, a competitive carbon price for Rochester is $43/t $CO_{2,\,eq}$ mitigated. At this carbon price, an HTC plant in Rochester would break even. Figure 2d shows the range of hypothetical carbon prices across NYS. Similar prices ($55−315/t $CO_{2,\,eq}$) were obtained by Shahid and Hittinger in their evaluation of FW anaerobic co-digestion.[28] By comparison, the average fourth quarter 2021 Low Carbon Fuel Standard (LCFS) credit was $177/t $CO_{2,eq}$.[54] While the LCFS is a California-based transportation fuel standard, it is a useful comparison to help policy makers assess the value of carbon mitigation to establish a competitive carbon market in NYS for electric and heating sector fuels.

Economic and Environmental Tradeoffs for HTC Plant Siting. Plant location and number can be optimized through any of the performance metrics evaluated in this study (i.e., NPV, MSP, CI, etc.). The distance between optimal locations is set as twice the r_{buffer} (40.2 km) to provide FW producers with only one option for redirection. Figure 4 shows

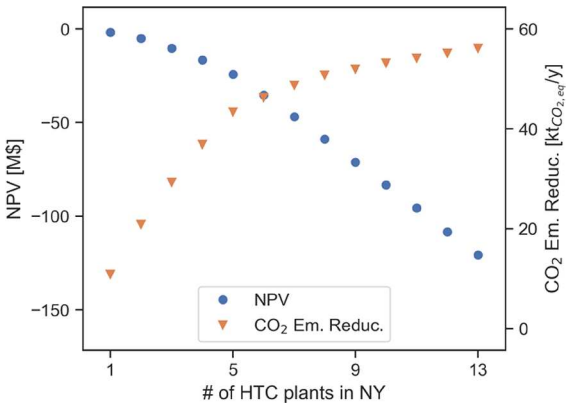

Figure 4. Overall economic (NPV) and environmental (emissions) performance of the set of HTC plants in NYS as a function of the number of HTC biorefineries increases.

the tradeoff between economic and environmental indicators as a function of number of biorefineries. More biorefineries enhance emissions reductions but requires more capital investment, decreasing the NPV. A system of five distributed HTC plants in Rochester, Buffalo, Albany, Syracuse, and White Plains (Figure 1) processing a combined 347 t/day FW (71% SRU, 4% DCW, and 25% BSG) can potentially generate 87 GWh/y of electricity, representing 41% of NYS's 2020 oil-fired electricity generation,[52] and contribute to a 43 kt $CO_{2,eq}$/y reduction (Figure 4) at an average carbon intensity of −0.34 t

https://doi.org/10.1021/acssuschemeng.2c04188
ACS Sustainable Chem. Eng. 2022, 10, 16578−16587

$CO_{2,eq}$/t FW. With an estimated NYS annual total FW generation of 4 Mt[37] (including additional FW sources), a system of distributed HTC biorefineries under the base case scenario could reduce emissions by 1.36 Mt $CO_{2,eq}$/y, representing around 13% of the state's landfill emissions. As such, the HTC system should not be viewed just as an energy producer. It offers a pathway to sustainable waste management and resource recovery that reduces GHG emissions.

The system of five distributed HTC plants results in a total NPV of −24 M$ (Figure 4). A higher number of centralized HTC clusters implies that less FW would be allocated to each cluster, reducing tipping fee revenues, HC generation, and carbon mitigation potential at the plant level, explaining the steeper decline in NPV and significant decrease in the incremental CO_2 reduction benefits beyond the fifth plant. This highlights the importance of carbon credits and financial incentives in achieving positive NPVs. The $MSP_{HC,eff}$ at the five biorefineries ranged from $47 to $171/t. The MSP_{HC}, independent of tipping fee revenues, ranged from $408 to $479/t, underscoring the importance of tipping fees in project profitability.

Enhancing Economic Feasibility through Policy and Process (Sensitivity). The base case analysis was limited to FW producers subject to current NYS regulations (Table S8). Increasing the r_{buffer} and decreasing $\dot{m}_{min}$ increases the amount of FW available to biorefineries, concomitantly increasing transportation costs and emissions. To measure the effects of HTC operating conditions, regulatory constraints, and economic parameters on NPV and net CO_2 emissions, a sensitivity analysis was performed by varying the base case parameters as shown in Table S9. The results of the sensitivity analysis for the HTC plant in Rochester (43.080 and −77.575) are shown in Figure 5.

The tipping fee has the highest impact on NPV; a 50% increase (parameter level 1) in tipping fee increases the base case NPV (−3 M$) by Δ = 12 M$ (Figure 5a). Decreasing the tipping fee by 50% decreases the NPV similarly. Given that (i) tipping fees constitute the main revenue streams for an HTC plant (Figure 3b) and (ii) the high sensitivity of the NPV to tipping fees, it is important for an HTC plant to balance economic gains and commercial attractiveness; high tipping fees would encourage FW generators to find alternative disposal options.

The second most impactful parameter on the NPV is the r_{buffer}. Increasing r_{buffer} increases the availability of waste streams, resulting in higher HC generation and tipping fee revenues. Increasing r_{buffer} also increases feedstock transportation costs and HTC capital costs. However, the rate at which revenues increase (linearly) outpaces the capital cost growth due to economies of scale (power scaling function as defined in eq 6). Further details on NPV and net CO_2 reduction as a function of r_{buffer} and $\dot{m}_{min}$ are available in Figure S5. Similarly, decreasing $\dot{m}_{min}$ (assuming a fixed r_{buffer}) captures more small-scale FW producers across NYS, resulting in higher tipping fees and economies of scale, ultimately increasing the NPV. Decreasing $\dot{m}_{min}$ to 0.36 t/week (parameter level 2) increases the base case NPV by Δ = 4.8 M$, to a net positive value of 1.8 M$, while increasing the $\dot{m}_{min}$ to 3.3 t/week (parameter level 2) decreases the base case NPV by Δ = −2 M$ to a total negative NPV of −5 M$.

Market-dependent parameters such as the discount rate, labor rate, HC selling price, and utilities costs impact the NPV to a lesser extent than the r_{buffer} and tipping fees. Reduction in

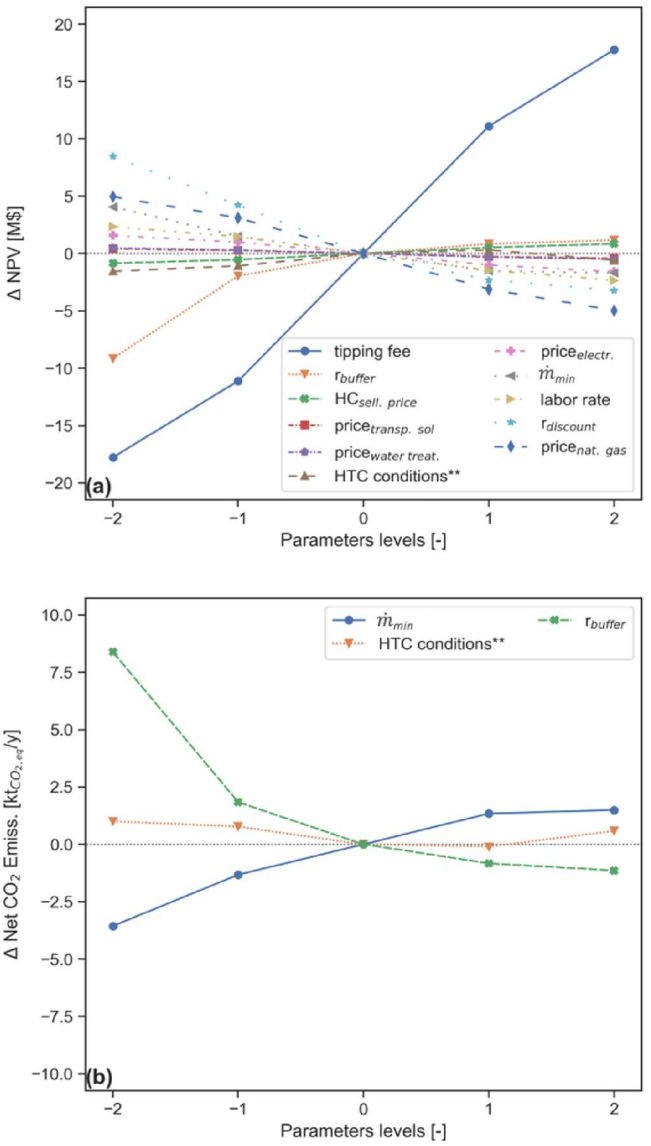

Figure 5. Sensitivity analysis of the effect of selected techno-economic parameters, regulatory constraints, and HTC conditions on NPV (a) and net CO_2 emissions (b), for a hypothetical HTC plant in Rochester.

NPV due to higher discount rates and utilities prices can be countered with corresponding changes in r_{buffer} and tipping fees, both of which are set by the plant operators. The small impact of the HC selling price and low HC generation reinforces the idea that the HTC plant should be primarily viewed as a waste treatment and carbon mitigation solution, rather than an energy recovery system. Finally, the price volatility of natural gas can have a significant impact on NPV as heat imports represent the second-highest component of the operating costs (Figure 3b).

Similar trends appear with net carbon emissions, where a higher r_{buffer} and lower $\dot{m}_{min}$ increase the amount of FW diverted from landfills, and result in more avoided emissions (Figure 5b). Implementing a policy changing $\dot{m}_{min}$ and r_{buffer} requirements to 72.4 km (parameter level 2) and 0.36 t/week (parameter level 2) would decrease emissions by 1.4 and 3.7 kt $CO_{2,eq}$/y, from their base case values, respectively, highlighting the importance of policy in enabling positive climate action and competitive mitigation strategies. Although HTC operat-

https://doi.org/10.1021/acssuschemeng.2c04188
ACS Sustainable Chem. Eng. 2022, 10, 16578−16587

ing conditions effect Y_{HC} and HHV_{HC}, their effect on NPV and net CO_2 emissions is much smaller compared to changes in regulatory constraints and economic parameters (Figure 5a and b).

CONCLUSIONS

A GIS-based computational model was developed to evaluate the spatial performance of a network of distributed biorefineries across New York State (NYS) to manage food waste (FW) using hydrothermal carbonization (HTC). HTC reduces greenhouse gas emissions associated with FW landfilling and generates energy in the form of a solid hydrochar that can be used as a substitute for coal in power applications. Under current NYS FW diversion legislation, large producers (>1.8 t/week) are required to redirect FW if they are within 40.2 km of a treatment facility. Although this represents a commercialization opportunity for HTC biorefineries, under current average coal prices, it does not provide a sufficient scale (in terms of eligible FW producers) to enable economically competitive HTC systems. The analysis showed that modifying regulations (lowering the 1.8 t/week minimum and increasing the 40.2 km buffer radius) can turn subsidy-dependent systems into profit-generating biorefineries. The model developed in this study enables policy makers to make informed decisions about the magnitude of regulatory changes needed to achieve meaningful climate action. The model computes carbon prices needed to establish a competitive market for food waste diversion technologies, ultimately serving as a foundation for a carbon-based standard or credit system in New York State. Finally, this model allows user modification of process inputs and parameters for future applicability. EPA's Excess Food Opportunities The map is a potential next step for readers interested in applying this model to other geographic regions and feedstocks.

ASSOCIATED CONTENT

Supporting Information

The Supporting Information is available free of charge at https://pubs.acs.org/doi/10.1021/acssuschemeng.2c04188.

Capital and operating cost estimation, discounted cash flow model development, landfill emission calculations, a description of databases consulted, and instructions to access our computational codes (PDF)

AUTHOR INFORMATION

Corresponding Author

Jillian L. Goldfarb − *Department of Biological and Environmental Engineering, Cornell University, Ithaca, New York 14853, United States;* orcid.org/0000-0001-8682-9714; Phone: 607 255 5789; Email: goldfarb@cornell.edu

Authors

Nazih Kassem − *Department of Biological and Environmental Engineering, Cornell University, Ithaca, New York 14853, United States; Smith School of Chemical and Biomolecular Engineering, Cornell University, Ithaca, New York 14853, United States*

Matteo Pecchi − *Department of Biological and Environmental Engineering, Cornell University, Ithaca, New York 14853, United States; Smith School of Chemical and Biomolecular Engineering, Cornell University, Ithaca, New York 14853, United States; Faculty of Science and Technology, Free University of Bolzano, Bolazano 39100, Italy;* orcid.org/0000-0002-0277-4304

Alex R. Maag − *Department of Biological and Environmental Engineering, Cornell University, Ithaca, New York 14853, United States; Department of Chemical Engineering, Worcester Polytechnical Institute, Worcester, Massachusetts 01609, United States*

Marco Baratieri − *Faculty of Science and Technology, Free University of Bolzano, Bolazano 39100, Italy*

Jefferson W. Tester − *Smith School of Chemical and Biomolecular Engineering, Cornell University, Ithaca, New York 14853, United States*

Complete contact information is available at: https://pubs.acs.org/10.1021/acssuschemeng.2c04188

Author Contributions

Conceptualization: J.L.G. Experimental work: M.P. and A.R.M. Computational model: N.K. and M.P. Writing - original draft: N.K. and M.P. Writing - revisions and editing: J.W.T., M.B., and J.L.G. Resources and supervision: J.W.T., M.B., and J.L.G.

Notes

The authors declare no competing financial interest.

ACKNOWLEDGMENTS

This work was supported by a Hatch Grant under accession no. 1021398 from the USDA National Institute of Food and Agriculture and by the National Science Foundation under grant no. CBET-2031916.

REFERENCES

(1) Crippa, M.; Solazzo, E.; Guizzardi, D.; Monforti-Ferrario, F.; Tubiello, F. N.; Leip, A. Food Systems Are Responsible for a Third of Global Anthropogenic GHG Emissions. *Nat. Food* **2021**, *2*, 198−209.

(2) US EPA. *National Overview: Facts and Figures on Materials, Wastes and Recycling.* https://www.epa.gov/facts-and-figures-about-materials-waste-and-recycling/national-overview-facts-and-figures-materials (accessed 2022-02-16).

(3) US EPA. *Basic Information about Landfill Gas.* https://www.epa.gov/lmop/basic-information-about-landfill-gas (accessed 2020-07-15).

(4) Springmann, M.; Clark, M.; Mason-D'Croz, D.; Wiebe, K.; Bodirsky, B. L.; Lassaletta, L.; de Vries, W.; Vermeulen, S. J.; Herrero, M.; Carlson, K. M.; Jonell, M.; Troell, M.; DeClerck, F.; Gordon, L. J.; Zurayk, R.; Scarborough, P.; Rayner, M.; Loken, B.; Fanzo, J.; Godfray, H. C. J.; Tilman, D.; Rockström, J.; Willett, W. Options for Keeping the Food System within Environmental Limits. *Nature* **2018**, *562*, 519−525.

(5) Van Vuuren, D. P.; Bijl, D. L.; Bogaart, P.; Stehfest, E.; Biemans, H.; Dekker, S. C.; Doelman, J. C.; Gernaat, D. E. H. J.; Harmsen, M. Integrated Scenarios to Support Analysis of the Food−Energy−Water Nexus. *Nat. Sustainability* **2019**, *2*, 1132−1141.

(6) New York State Department of Environmental Conservation. *Food Donation and Food Scraps Recycling Law.* https://www.dec.ny.gov/chemical/114499.html (accessed 2022-02-16).

(7) Badgett, A.; Milbrandt, A. Food Waste Disposal and Utilization in the United States: A Spatial Cost Benefit Analysis. *J. Cleaner Prod.* **2021**, *314*, No. 128057.

(8) Gómez-Sanabria, A.; Kiesewetter, G.; Klimont, Z.; Schoepp, W.; Haberl, H. Potential for Future Reductions of Global GHG and Air Pollutants from Circular Waste Management Systems. *Nat. Commun.* **2022**, *13*, 1−12.

(9) Hagos, K.; Zong, J.; Li, D.; Liu, C.; Lu, X. Anaerobic Co-Digestion Process for Biogas Production: Progress, Challenges and Perspectives. *Renewable Sustainable Energy Rev.* **2017**, *76*, 1485−1496.

(10) Naqvi, S. R.; Tariq, R.; Hameed, Z.; Ali, I.; Naqvi, M.; Chen, W.-H.; Ceylan, S.; Rashid, H.; Ahmad, J.; Taqvi, S. A.; Shahbaz, M. Pyrolysis of High Ash Sewage Sludge: Kinetics and Thermodynamic Analysis Using Coats-Redfern Method. *Renewable Energy* **2019**, *131*, 854−860.
(11) Peng, W.; Lü, F.; Hao, L.; Zhang, H.; Shao, L.; He, P. Digestate Management for High-Solid Anaerobic Digestion of Organic Wastes: A Review. *Bioresour. Technol.* **2020**, *297*, No. 122485.
(12) Libra, J. A.; Ro, K. S.; Kammann, C.; Funke, A.; Berge, N. D.; Neubauer, Y.; Titirici, M. M.; Fühner, C.; Bens, O.; Kern, J.; Emmerich, K. H. Hydrothermal Carbonization of Biomass Residuals: A Comparative Review of the Chemistry, Processes and Applications of Wet and Dry Pyrolysis. *Biofuels* **2011**, *2*, 71−106.
(13) Funke, A.; Ziegler, F.Hydrothermal Carbonization of Biomass: A Summary and Discussion of Chemical Mechanisms for Process Engineering. *Biofuels, Bioproducts and Biorefining*. John Wiley & Sons, Ltd. March 2010, pp. 160−177. DOI: 10.1002/bbb.198.
(14) Rodriguez Correa, C.; Bernardo, M.; Ribeiro, R. P. P. L.; Esteves, I. A. A. C.; Kruse, A. Evaluation of Hydrothermal Carbonization as a Preliminary Step for the Production of Functional Materials from Biogas Digestate. *J. Anal. Appl. Pyrolysis* **2017**, *124*, 461−474.
(15) Pauline, A. L.; Joseph, K. Hydrothermal Carbonization of Organic Wastes to Carbonaceous Solid Fuel − A Review of Mechanisms and Process Parameters. *Fuel* **2020**, *279*, No. 118472.
(16) Islam, M. A.; Limon, M. S. H.; Romić, M.; Islam, M. A. Hydrochar-Based Soil Amendments for Agriculture: A Review of Recent Progress. *Arab. J. Geosci.* **2021**, *14*, 102.
(17) Celletti, S.; Bergamo, A.; Benedetti, V.; Pecchi, M.; Patuzzi, F.; Basso, D.; Baratieri, M.; Cesco, S.; Mimmo, T. Phytotoxicity of Hydrochars Obtained by Hydrothermal Carbonization of Manure-Based Digestate. *J. Environ. Manage.* **2021**, *280*, No. 111635.
(18) González-Arias, J.; Baena-Moreno, F. M.; Sánchez, M. E.; Cara-Jiménez, J. Optimizing Hydrothermal Carbonization of Olive Tree Pruning: A Techno-Economic Analysis Based on Experimental Results. *Sci. Total Environ.* **2021**, *784*, No. 147169.
(19) Akbari, M.; Oyedun, A. O.; Kumar, A. Comparative Energy and Techno-Economic Analyses of Two Different Configurations for Hydrothermal Carbonization of Yard Waste. *Bioresour. Technol. Rep.* **2019**, *7*, No. 100210.
(20) Lucian, M.; Fiori, L. Hydrothermal Carbonization of Waste Biomass: Process Design, Modeling, Energy Efficiency and Cost Analysis. *Energies* **2017**, *10*, 211.
(21) González-Arias, J.; Sánchez, M. E.; Cara-Jiménez, J. Profitability Analysis of Thermochemical Processes for Biomass-Waste Valorization: A Comparison of Dry vs Wet Treatments. *Sci. Total Environ.* **2022**, *811*, No. 152240.
(22) Unrean, P.; Lai Fui, B. C.; Rianawati, E.; Acda, M. Comparative Techno-Economic Assessment and Environmental Impacts of Rice Husk-to-Fuel Conversion Technologies. *Energy* **2018**, *151*, 581−593.
(23) Mahmood, R.; Parshetti, G. K.; Balasubramanian, R. Energy, Exergy and Techno-Economic Analyses of Hydrothermal Oxidation of Food Waste to Produce Hydro-Char and Bio-Oil. *Energy* **2016**, *102*, 187−198.
(24) Saha, N.; McGaughy, K.; Davis, S. C.; Reza, M. T. Assessing Hydrothermal Carbonization as Sustainable Home Sewage Management for Rural Counties: A Case Study from Appalachian Ohio. *Sci. Total Environ.* **2021**, *781*, No. 146648.
(25) Do, T. X.; Phan, T. T. N.; Van Dinh Son, T. Process Modeling and Economic Assessment of Converting Municipal Solid Waste into Solid Fuel via Hydrothermal Processing: A Case Study in Vietnam. *J. Mater. Cycles Waste Manage.* **2021**, *23*, 2318−2335.
(26) Medina-Martos, E.; Istrate, I.-R.; Villamil, J. A.; Gálvez-Martos, J.-L.; Dufour, J.; Mohedano, Á. F. Techno-Economic and Life Cycle Assessment of an Integrated Hydrothermal Carbonization System for Sewage Sludge. *J. Cleaner Prod.* **2020**, *277*, No. 122930.
(27) Saba, A.; McGaughy, K.; Reza, M. Techno-Economic Assessment of Co-Hydrothermal Carbonization of a Coal-Miscanthus Blend. *Energies* **2019**, *12*, 630.
(28) Shahid, K.; Hittinger, E. Techno-Economic Optimization of Food Waste Diversion to Treatment Facilities to Determine Cost Effectiveness of Policy Incentives. *J. Cleaner Prod.* **2021**, *279*, No. 122634.
(29) New York State Pollution Prevention Institute. *Organic Resource Locator | New York State Pollution Prevention Institute | RIT*. https://www.rit.edu/affiliate/nysp2i/organic-resource-locator (accessed 2021-12-01).
(30) Kassem, N.; Sills, D.; Posmanik, R.; Blair, C.; Tester, J. W. Combining Anaerobic Digestion and Hydrothermal Liquefaction in the Conversion of Dairy Waste into Energy: A Techno Economic Model for New York State. *Waste Manage.* **2020**, *103*, 228−239.
(31) Pecchi, M.; Baratieri, M.; Goldfarb, J. L.; Maag, A. R. Effect of Solvent and Feedstock Selection on Primary and Secondary Chars Produced via Hydrothermal Carbonization of Food Wastes. *Bioresour. Technol.* **2022**, *348*, No. 126799.
(32) Saqib, N. U.; Sharma, H. B.; Baroutian, S.; Dubey, B.; Sarmah, A. K. Valorisation of Food Waste via Hydrothermal Carbonisation and Techno-Economic Feasibility Assessment. *Sci. Total Environ.* **2019**, *690*, 261−276.
(33) Michailos, S.; Walker, M.; Moody, A.; Poggio, D.; Pourkashanian, M. A Techno-Economic Assessment of Implementing Power-to-Gas Systems Based on Biomethanation in an Operating Waste Water Treatment Plant. *J. Environ. Chem. Eng.* **2021**, *9*, No. 104735.
(34) New York State Department of Labor. *Occupational Wages*. https://statistics.labor.ny.gov/lswage2.asp#51-0000 (accessed 2022-02-03).
(35) New York State Energy Research and Development Authority. *Monthly Average Retail Price of Electricity - Industrial - NYSERDA*. https://www.nyserda.ny.gov/Researchers-and-Policymakers/Energy-Prices/Electricity/Monthly-Avg-Electricity-Industrial (accessed 2022-02-03).
(36) New York State Energy Research and Development Authority. *Monthly Average Price of Natural Gas - Industrial - NYSERDA*. https://www.nyserda.ny.gov/Researchers-and-Policymakers/Energy-Prices/Natural-Gas/Monthly-Average-Price-of-Natural-Gas-Industrial (accessed 2022-02-03).
(37) Manson, C.*Benefit-Cost Analysis of Potential Food Waste Diversion Legislation*; New York State Energy Research and Development Authority2017, No. March.
(38) Harrigan, T. M. Liquid Manure Hauling Capacity of Custom Applicators Using Tank Spreader Systems. *Appl. Eng. Agric.* **2010**, *26*, 729−741.
(39) Saralyn, Bunch; Peterson, J.; Poehlman, E.; Loper, S.; Wilburn, M.*Water and Wastewater Annual Price Escalation Rates for Selected Cities across the United States*; U.S. Energy Information Administration2017.
(40) U.S. Energy Information Administration. *New York - State Energy Profile Analysis - U.S. Energy Information Administration (EIA)*. https://www.eia.gov/state/analysis.php?sid=NY(accessed 2022-03-16).
(41) U.S. Energy Information Administration. *Coal Data Browser - Average price by rank*. https://www.eia.gov/coal/data/browser/#/topic/29?agg=0,1&geo=nvg1qag9vvlpg&rank=l&freq=A&start=2001&end=2020&ctype=linechart&ltype=pin&rtype=s&maptype=0&rse=0&pin= (accessed 2022-02-10).
(42) Environmental Research & Education Foundation. *Analysis of MSW Landfill Tipping Fees-2020*; EREF2021.
(43) US EPA. *Landfill Technical Data*. https://www.epa.gov/lmop/landfill-technical-data (accessed 2022-02-11).
(44) US EPA. *eGRID Data Explorer*. https://www.epa.gov/egrid/data-explorer (accessed 2022-03-16).
(45) U.S. Energy Information Administration. *New York Natural Gas Summary*. https://www.eia.gov/dnav/ng/ng_sum_lsum_dcu_SNY_a.htm (accessed 2022-02-11).
(46) U.S. Energy Information Administration. *State Carbon Dioxide Emissions Data*. https://www.eia.gov/environment/emissions/state/ (accessed 2022-02-11).

(47) US EPA. *Emission Factors for Greenhouse Gas Inventories*; US EPA2018.
(48) IPCC. *Climate Change 2014: Synthesis Report, IPCC Fifth Assessment Report*; Geneva, 2014.
(49) US EPA Climate Change Division. *Inventory of U.S. Greenhouse Gas Emissions and Sinks: 1990−2019 − Main Text - Corrected Per Corrigenda*; US EPA Updated 05/2021. 2021.
(50) Bardhan, M.; Novera, T. M.; Tabassum, M.; Islam, M. A.; Islam, M. A.; Hameed, B. H. Co-Hydrothermal Carbonization of Different Feedstocks to Hydrochar as Potential Energy for the Future World: A Review. *J. Cleaner Prod.* **2021**, *298*, No. 126734.
(51) US Department of Energy. *Transformative Power Systems | Department of Energy*. https://www.energy.gov/fecm/science-innovation/office-clean-coal-and-carbon-management/advanced-energy-systems/transformative (accessed 2022-03-16).
(52) NYISO. *New York's Clean Energy Grid of the Future - Power Trends 2021*; 2021.
(53) New York State Energy Research and Development Authority. *New York State Greenhouse Gas Inventory : 1990−2016*; 2019.
(54) California Air Resources Board. *Monthly LCFS Credit Transfer Activity Reports*. https://ww2.arb.ca.gov/resources/documents/monthly-lcfs-credit-transfer-activity-reports (accessed 2022-03-17).

https://doi.org/10.1021/acssuschemeng.2c04188
ACS Sustainable Chem. Eng. 2022, 10, 16578−16587